Atomic bonding and electronic stability of the binary sigma phase

Wei Liu, Xiao-Gang Lu, Qing-Miao Hu, Hao Wang, Yi Liu, Pascal Boulet, Marie-Christine Record

Atomic bonding and electronic stability of the binary sigma phase

LIU Wei [1], LU Xiao-Gang [1, 2], HU Qing-Miao [3, *], WANG Hao [2,*], LIU Yi [1], BOULET Pascal [4], RECORD Marie-Christine [5]

[1] Materials Genome Institute, Shanghai University, 99 Shangda Raod, Shanghai 200444, China

[2] School of Materials Science and Engineering, Shanghai University, 99 Shangda Raod, Shanghai 200444, China

[3] Titanium Alloy Laboratory, Institute of Metal Research, Chinese Academy of Sciences, 72 Wenhua Road, Shenyang 110016, China

[4] Aix-Marseille Université, CNRS, MADIREL, 52 Avenue Escadrille Normandie Niemen, Marseille 13013, France

[5] Aix-Marseille Université, Université de Toulon, CNRS, IM2NP, Marseille 13013, France

*Corresponding author: qmhu@imr.ac.cn (Hu Q-M); haowang@i.shu.edu.cn (Wang H)
tianziben@163.com (Liu W)
xglu@t.shu.edu.cn (Lu X-G);
yiliu@t.shu.edu.cn (Liu Y)
pascal.boulet@univ-amu.fr (Boulet P)
m-c.record@univ-amu.fr (Record M-C)

Abstract

The formation of the sigma phase in technologically important materials influences greatly their mechanical properties. Fundamental knowledge on the sigma phase is demanded to understand the phase stability and reasonably control its precipitation. The present work clarifies the atomic bonding characteristics of the binary sigma phase including *A*-Al (*A*=Nb, Ta) and transition metal systems (TM-TM) based on the electronic density of states (DOS) and electron localization function (ELF) calculated by using first-principles methods. We show that the atomic bonds of the binary sigma phase exhibit both metallic and covalent characters. The covalent bonding for *A*-Al (*A*=Nb, Ta) is stronger than that for TM-TM. Additionally, the completely ordered $A_{66.7}Al_{33.3}$ (*A*=Nb, Ta) sigma compounds bear higher electronic stability than the disorder compounds. Besides, for a TM-TM sigma compound, the constituent atom with more electron shells or less valence electrons holds stronger atomic bondings. When increasing its atomic occupancy on a specific site, the atomic bonding on the site increases.

Keywords: A. sigma phase, C. atomic bonding, C. electronic stability, C. DOS, C. ELF, D. first-principles calculations.

1. Introduction

The sigma phase is a non-stoichiometric intermetallic compound, that crystallizes in a tetragonal structure with 30 atoms distributed on five nonequivalent sites denoted as 2*a*, 4*f*, 8i_1, 8i_2 and 8*j* [1–3] (see Fig. 1). It mostly forms in transition element systems, but it also exists in two systems containing

a main-group element, i.e., *A*-Al (*A*=Nb, Ta). The sigma phase has attracted great experimental and theoretical research interests. The thermodynamic [4,5] and molar volume [6] databases of the sigma phase were built successively to predict the precipitation and molar volume of the sigma phase in multicomponent systems by using the CALPHAD method [7–9]. Physical properties of the sigma phase, such as site occupancy [2,10,11], elastic properties [12], molar volume [13], enthalpy of formation [14,15] and magnetism [16,17] have drawn significant concern as well.

Electronic structure analyses are effective approaches to explore the physical and crystallographic properties as well as the stability [14] of the sigma phase. Berne et al. [18] reported that coordination number 12 (CN12) sites are preferable for atoms with filled, nearly filled or empty *d* shells. The reason is that CN12 sites have approximately icosahedral symmetry, causing high degeneracy of *d*-like electronic levels [18,19]. Grånäs et al. [20] proposed that, for Mo-Ru sigma compounds, Mo atoms prefer to occupy large CN sites, favoring the stronger covalent bonding between atoms.

In the present work, the first principles plane wave pseudo-potential method and exact muffin-tin orbitals method in combination with coherent potential approximation were used to reveal the bonding between atoms of the sigma phase. To facilitate explanation, all the studied binary sigma compounds were designated as *A*-*B*, where atom *A* has a larger atomic size than atom *B*. The ordered and disordered state is designated with atomic occupancy as presented in Table 1.

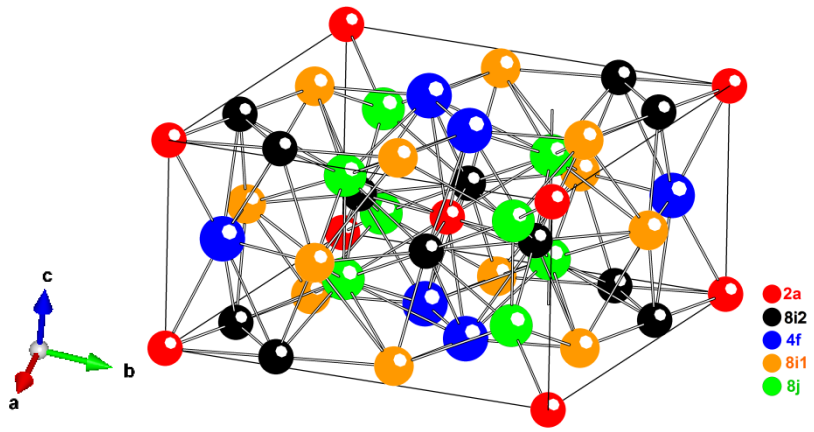

Fig. 1. Crystal structure of the sigma phase. Atoms occupying different Wyckoff positions (i.e., 2*a*, 4*f*, 8i_1, 8i_2 and 8*j*) are indicated by different colors. (Color online).

Table 1 Site occupancies of the completely ordered A_2B and disordered A_xB_{1-x} sigma compounds.

Wyckoff position	2a	4f	$8i_1$	$8i_2$	8j
Coordination number (CN)	12	15	14	12	14
Completely ordered state (A_2B) [2]	0	1	1	0	1
Disordered state (A_xB_{1-x})	x	x	x	x	x

2. Methodology and calculation details

First-principles calculations were performed by using the exact muffin-tin orbitals method in combination with coherent potential approximation (EMTO-CPA) and plane wave pseudo-potential method implemented in the Vienna *ab initio* simulation package (VASP). The EMTO-CPA method was adopted mainly to deal with chemical disordered sigma compounds. By using this method, we can conveniently obtain the electronic density of states (DOS) for the sigma compounds with different atomic occupancies on lattice sites. We used VASP to calculate the electron localization function (ELF) for the completely ordered sigma compounds. The calculation details are as follows.

2.1. EMTO-CPA calculations

The Green's function technique is used to solve the one electron Kohn-Sham equation within the exact muffin-tin orbitals (EMTO) method [21,22]. The optimized overlapping muffin-tin approximation is conducted when dealing with the effective potential in the one-electron equation. Additionally, the full charge density (FCD) method [21] is used to correct the total energy. The wave function is expanded by using the basis sets of the exact muffin-tin orbitals [21,22]. The coherent potential approximation (CPA) [23–25] is incorporated within the EMTO code, which facilitates the calculations dealing with chemical disordered alloys.

In the present work, Green's function was calculated for 16 complex energy points distributed exponentially on a semicircular contour. We adopted the scalar-relativistic and soft-core approximations. The electronic exchange-correlation functional within the generalized-gradient approximation (GGA) as parameterized by Perdew et al. [26] was used. The Brillouin zone was sampled by a uniform k-point mesh (3×3×6) without any smearing technique. The DOS were obtained at the equilibrium volume.

2.2. VASP calculations

The plane wave method with projector augmented wave (PAW) pseudo-potentials [27] based on density-functional theory (DFT) [28] is implemented in VASP [29]. The exchange-correlation functional within the generalized gradient approximation (GGA) as parameterized by Perdew and

Wang namely GGA-PW91 [30] was employed. The plane-wave cutoff energy was set as 400 eV. The k-point meshes (8×8×15) for Brillouin zone sampling were constructed using the Monkhorst–Pack scheme [31]. To facilitate the calculations, ZenGen script-tool [32] was used to automatically generate input files. The ELF was obtained using the relaxed structure at the equilibrium volume.

3. Results and discussion

In order to gain better understanding of the chemical bonding in the sigma phase, both electronic density of states (DOS) and electron localization function (ELF) calculations were conducted for several binary sigma phase systems. The calculation results indicate that the atomic bonds of the sigma phase exhibit both metallic and covalent characters for both *A*-Al (*A*=Nb, Ta) and transition metal systems (TM-TM). The covalent bonding for *A*-Al (*A*=Nb, Ta) is stronger than that for TM-TM.

3.1. Electronic stability of *A*-Al (*A*=Nb, Ta) sigma systems

To clarify the electronic stability of *A*-Al (*A*=Nb, Ta) sigma systems, the total electronic density of states (TDOS) of the $Nb_{65.9}Al_{34.1}$, $Nb_{66.7}Al_{33.3}$, $Ta_{65.5}Al_{34.5}$, $Ta_{66.7}Al_{33.3}$ and $Ta_{75.6}Al_{24.4}$ sigma compounds were computed with the site occupancies taken from literature [2,33–35] as presented in Fig. 2. We can observe that for all the compounds, the TDOS at the Fermi level are finite, which indicates metallic bonding between atoms. For $Nb_{65.9}Al_{34.1}$, $Nb_{66.7}Al_{33.3}$, $Ta_{65.5}Al_{34.5}$ and $Ta_{66.7}Al_{33.3}$, the Fermi level falls within the pseudogap, which results from hybridization between the electronic states, and represents a covalent bonding between atoms [36,37]. Normally, covalent bonding is stronger than metallic bonding [36].

For the completely ordered $A_{66.7}Al_{33.3}$ (*A*=Nb, Ta) compounds, the pseudogaps at the Fermi level are deeper, and the densities of states at the Fermi level are smaller than that for $Nb_{65.9}Al_{34.1}$ or $Ta_{65.5}Al_{34.5}$/$Ta_{75.6}Al_{24.4}$ with atomic disorder. It indicates a stronger atomic bonding and thus a larger electronic stability for $A_{66.7}Al_{33.3}$ (*A*=Nb or Ta) than for other Nb-Al or Ta-Al configurations. Additionally, the completely ordered $A_{66.7}B_{33.3}$ (i.e., $B_{2a}A_{4f}A_{8i1}B_{8i2}A_{8j}$) compound holds a small mismatch between atom and lattice site, namely large atom *A* occupy large CN sites (i.e., 4*f*, 8i_1 and 8*j*); small atom *B* occupy small CN sites (i.e., 2*a*, 8i_2) [11]. Therefore both the electronic stability and size mismatch favor the stability of the completely ordered $A_{66.7}Al_{33.3}$ (*A*=Nb, Ta) compounds. Hence, the sigma compounds of *A*-Al (*A*=Nb, Ta) systems are observed experimentally to be highly ordered (see eg. Ref. [2,11] and references therein).

To further understand the electronic stability of the $A_{66.7}Al_{33.3}$ (A=Nb, Ta) compounds, we analyzed in detail their TDOS and partial DOS (PDOS) as presented~~, respectively,~~ in Figs. 2 and 3, respectively. We observe that the TDOS of $Ta_{66.7}Al_{33.3}$ shift to lower energy as compared to that of $Nb_{66.7}Al_{33.3}$ due to a stronger directional d bonding between Ta atoms [38].

Besides, there is a peak located at around -0.22 Ry for $Nb_{66.7}Al_{33.3}$ and -0.26 Ry for $Ta_{66.7}Al_{33.3}$, which comes from the bonding state made up of TM-d (TM=Nb, Ta) and Al-p orbitals [39] as can be observed from the PDOS in Fig. 3. The Nb(d)-Al(p) bonding state is more localized than Ta(d)-Al(p), as indicated by a steeper bonding peak for Nb(d)-Al(p). Next to the peak, slightly higher in energy, there is a drop of the density of states, as presented in Fig. 2. It is generated by the hybridization of the TM-d and Al-p orbitals [38].

Additionally, several small peaks appear on the top of the major bonding states just below the Fermi level from around -0.2 to 0 Ry. The first, energy-lowest small peak (at around -0.144 Ry for $Nb_{66.7}Al_{33.3}$ and -0.160 Ry for $Ta_{66.7}Al_{33.3}$) is mainly made up of TM-d and Al-p orbitals; the other small peaks correspond to the directional d bonding.

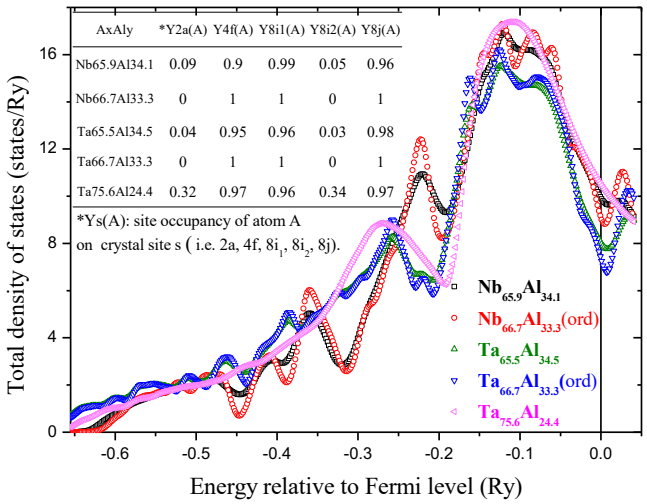

Fig. 2. Total electronic density of states (TDOS) for A-Al (A=Nb, Ta) sigma compounds from EMTO-CPA calculations. The site occupancies of the compounds, shown in the inserted Table in the figure, were adopted from the literature, namely Ref. [2] for $Nb_{65.9}Al_{34.1}$, Ref. [33] for $Nb_{66.7}Al_{33.3}$, Ref. [34] for $Ta_{65.5}Al_{34.5}$ Ref. [35] for $Ta_{66.7}Al_{33.3}$ and Ref. [34] for $Ta_{75.6}Al_{24.4}$. 'ord' represents the completely ordered state. The vertical line indicates the Fermi level. (Color online).

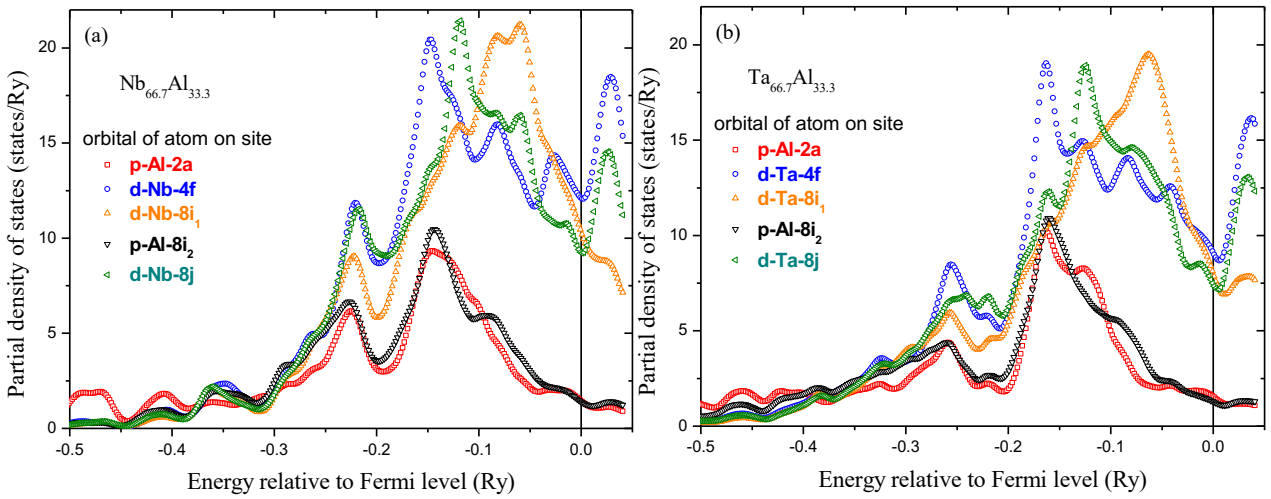

Fig. 3. Partial electronic density of states (PDOS) for the completely ordered $A_{66.7}Al_{33.3}$ (A=Nb, Ta) sigma compounds (i.e., $Al_{2a}A_{4f}A_{8i1}Al_{8i2}A_{8j}$) from EMTO-CPA calculations. The vertical line indicates the Fermi level. (Color online).

The ELF of the completely ordered $A_{66.7}Al_{33.3}$ (A=Nb, Ta) compounds were also calculated as presented in Fig. 4, where the range of ELF values is from 0 to 0.76. Theoretically, when ELF values equal 0.5, the Pauli repulsion at that position has the same value as in a uniform electron gas of the same density; when ELF values are close to 0 and 1, the local Pauli repulsion is very large and very small compared to that in a uniform electron gas [40], respectively. In other words, ELF=0.5 represents the electron-gas like pair probability; ELF=0 and ELF=1 represent perfect delocalization and localization, respectively [41]. For more details see Ref. [40,42]. In general, metallic bonding is supposed to be delocalized; covalent bonding is supposed to be localized [41,43].

For the completely ordered $A_{66.7}Al_{33.3}$ (A=Nb, Ta), where Nb and Ta occupy 4*f*, 8i_1, 8*j* sites, and Al occupy 2*a*, 8i_2 sites, the ELF results in Fig. 4 agree well with the previous DOS calculations in Figs. 2 and 3. We can observe from Fig. 4 that the Ta(*d*)-Ta(*d*) bonding regions are wider and with a relatively larger ELF value than Nb(*d*)-Nb(*d*). It indicates a stronger directional bonding between Ta atoms. Additionally, for $Nb_{66.7}Al_{33.3}$, the ELF values within Nb(*d*)-Al(*p*) and Al(*p*)-Al(*p*) bonding regions are slightly higher than that for $Ta_{66.7}Al_{33.3}$ indicating that the corresponding bonding regions of $Nb_{66.7}Al_{33.3}$ are more localized. Note that the Ta(*d*)-Al(*p*) bonding regions are slightly wider than Nb(*d*)-Al(*p*) ones.

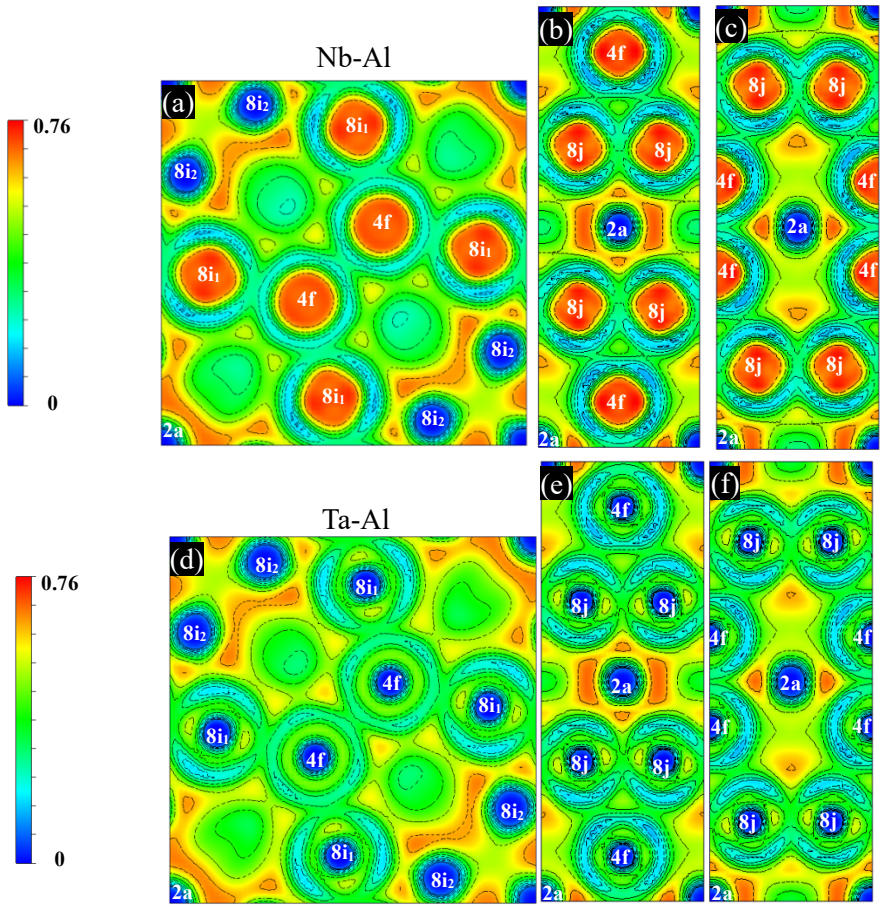

Fig. 4. Electron Localization Function (ELF) of the completely ordered $Nb_{66.7}Al_{33.3}$ (upper half) and $Ta_{66.7}Al_{33.3}$ (lower half) sigma compounds namely $Al_{2a}A_{4f}A_{8i1}Al_{8i2}A_{8j}$ (A=Nb, Ta). (a,d), (b,e) and (c,f) depict the ELF across (001), (110) and (-110) slice planes with distance from origin of 0 Å, 7.05 Å / 7.03 Å (Nb-Al/Ta-Al) and 0 Å, respectively. The color scale is given on the left. The scaling is between 0 and 0.76 (the maximum ELF for $Nb_{66.7}Al_{33.3}$ and $Ta_{66.7}Al_{33.3}$ is about 0.76 and 0.69, respectively). (Color online).

3.2. Influence of electronic configuration on atomic bonding for TM-TM sigma systems

To figure out the influence of electronic configuration, we calculated the DOS for Cr-Fe, Cr-Co, Re-Mn, Os-Cr, Re-Cr, Re-V, Ru-Cr, Mo-Mn, Mo-Re and Mo-Os binary sigma systems, but to avoid redundancy only the results of typical Cr-Fe, Mo-Re, Re-Mn and Re-V systems are shown in the present work.

The Cr-Fe system can serve as a prototype when investigating the influence of the valence electron factor on atomic bonding, where Fe ($3d^64s^2$) has two more valence electrons than Cr ($3d^54s^1$). Fig. 5 (a) presents the site-decomposed DOS of the two $Cr_{49.5}Fe_{50.5}$ sigma compounds one with site occupancies from the literature and the other in hypothetically disordered state. For clarity, only 2*a* and 4*f* sites are presented, as other sites also support the following argument. It indicates that when more Cr atoms occupy a specific crystal site, the atomic bonding on the site becomes stronger, which

manifest itself by a deeper pseudogap and a smaller density of states at the Fermi level.

The Re-Mn system can serve as a prototype when investigating the influence of the electron shell factor on atomic bonding, where Re ($5d^5 6s^2$) has two more electron shells than Mn ($3d^5 4s^2$). Fig. 5 (b) shows the site-decomposed DOS of the two $Re_{51.2}Mn_{48.8}$ sigma compounds one with site occupancies from the literature and the other in hypothetically disordered state. It indicates that when more Re atoms occupy a specific crystal site, the atomic bonding on the site becomes stronger.

In fact, the above arguments on Cr-Fe and Re-Mn are universal for the binary TM-TM sigma phase. For a TM-TM sigma compound, the constituent atom, with less valence electrons or more electron shells, holds higher electronic stability. When increasing its atomic occupancy on a specific site, the atomic bonding on the site becomes stronger.

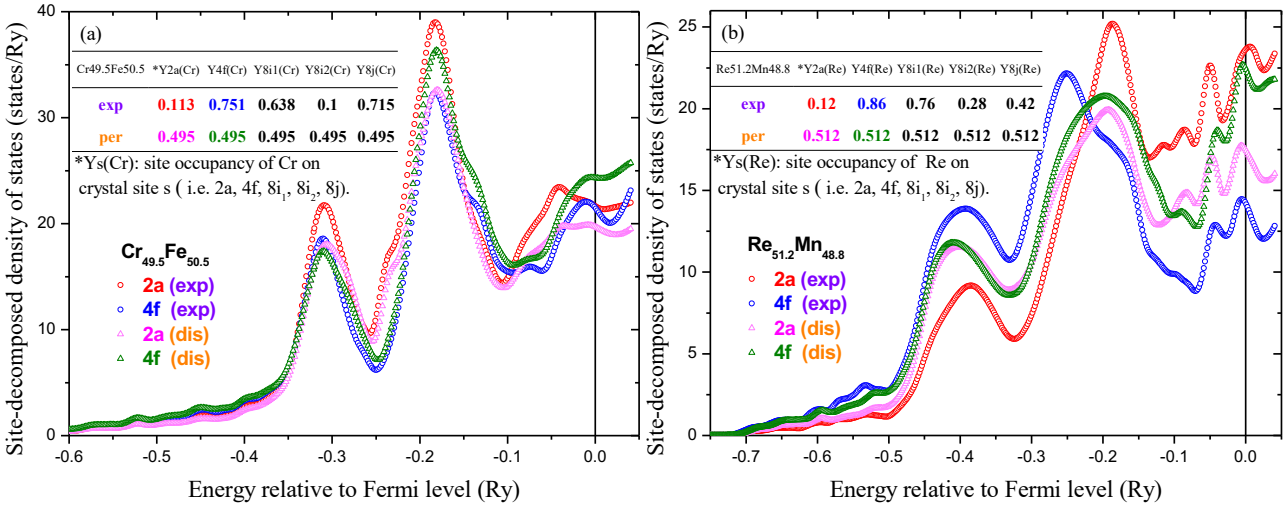

Fig. 5. Site-decomposed DOS for (a) Cr-Fe and (b) Re-Mn sigma compounds from EMTO-CPA calculations. 'exp' and 'dis' indicate compounds with site occupancies from the literature ($Cr_{49.5}Fe_{50.5}$ [44] and $Re_{51.2}Mn_{48.8}$ [2]) and in hypothetically disordered state, respectively. The vertical lines indicate the Fermi level. (Color online).

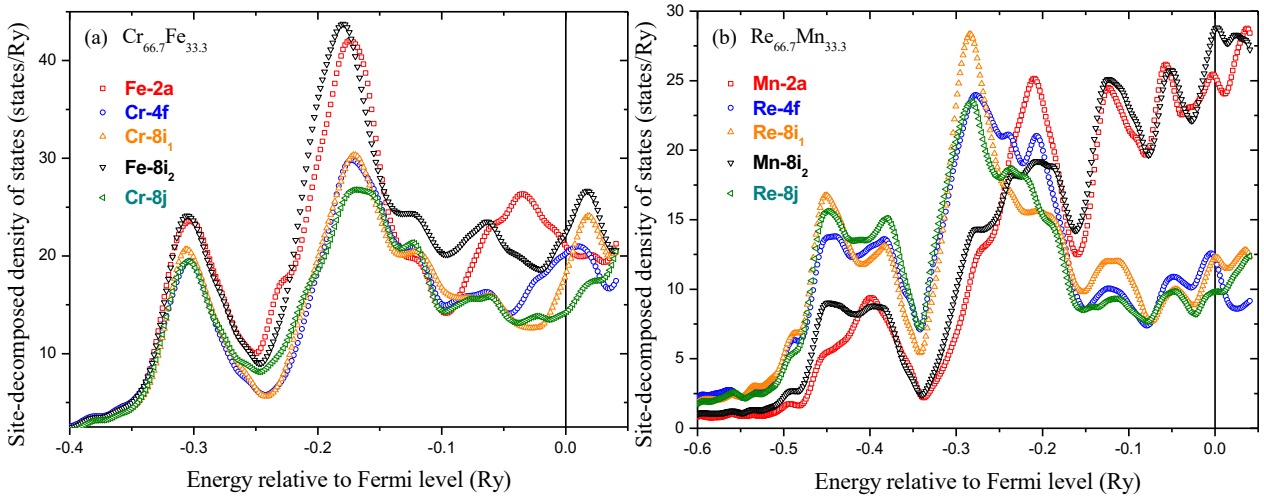

Fig. 6. Site-decomposed DOS for the completely ordered $Cr_{66.7}Fe_{33.3}$ and $Re_{66.7}Mn_{33.3}$ sigma compounds (i.e., $B_{2a}A_{4f}A_{8i1}B_{8i2}A_{8j}$) from EMTO-CPA calculations. The vertical lines indicate the Fermi level. (Color online).

To further validate the above statement, we calculated both the site-decomposed DOS and ELF for the completely ordered $Cr_{66.7}Fe_{33.3}$ and $Re_{66.7}Mn_{33.3}$ sigma compounds. The site-decomposed DOS in Fig. 6 indicate a stronger bonding between Cr atoms and a weaker bonding between Fe atoms for $Cr_{66.7}Fe_{33.3}$, and a stronger bonding between Re atoms and a much weaker bonding between Mn atoms for $Re_{66.7}Mn_{33.3}$. The above results agree well with the ELF calculations for $Cr_{66.7}Fe_{33.3}$ and $Re_{66.7}Mn_{33.3}$ shown in Figs. 7 and 8, respectively. Note that for the ELF of $Cr_{66.7}Fe_{33.3}$, the features of the outer-core region, spatially separated from the common valence region, is due to the unequal occupation of *d* orbital [40].

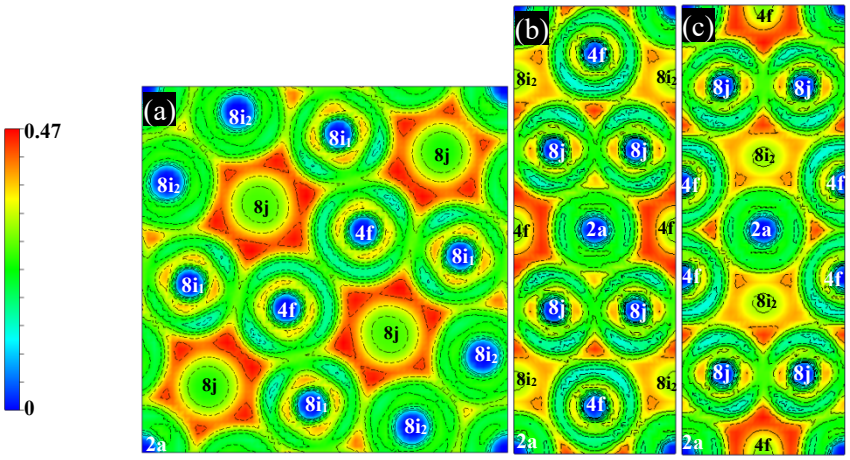

Fig. 7. Electron Localization Function (ELF) of the completely ordered $Cr_{66.7}Fe_{33.3}$ sigma compound namely $Fe_{2a}Cr_{4f}Cr_{8i1}Fe_{8i2}Cr_{8j}$. (a), (b) and (c) depict the ELF across (001), (110) and (-110) slice planes with distance from origin of 0 Å, 6.14 Å and 0 Å, respectively. The color scale is given on the left. The scaling is between 0 and 0.47. Crystal sites with white labels are in the slice planes crystal site with black labels are in upper or lower layers of the slice planes. (Color online).

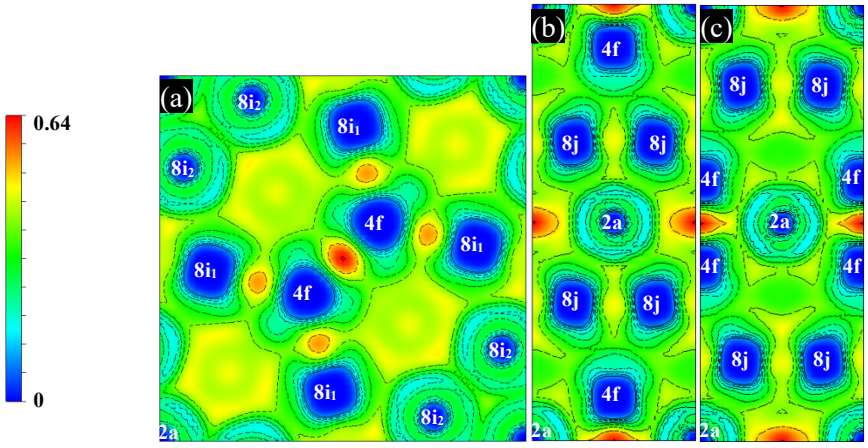

Fig. 8. Electron Localization Function (ELF) of the completely ordered $Re_{66.7}Mn_{33.3}$ sigma compound namely $Mn_{2a}Re_{4f}Re_{8i1}Mn_{8i2}Re_{8j}$. (a), (b) and (c) depict the ELF across (001), (110) and (-110) slice planes with distance from origin of 0 Å, 6.48 Å and 0 Å, respectively. The color scale is given on the left. The scaling is

between 0 and 0.64. (Color online).

3.3. Discussion

3.3.1. Site occupancy preference on CN12 sites of the sigma phase

Berne et al. [18] and then Crivello et al. [14] clarified that CN12 sites are preferable for atoms with filled, nearly filled or empty *d* shells, the reason being that CN12 sites have approximate icosahedral symmetry causing high degeneracy of electronic *d*-like levels [18,19]. Thus atoms with half-filled *d* shells would have high density of states when occupying CN12 sites and consequently occupy high CN sites [14]. However, the present calculations show disagreement with the above argument.

For Re-V sigma system, where Re ($5d^5 6s^2$) bears half-filled d shells, we calculated the site decomposed DOS of the two $Re_{78}V_{22}$ compounds with different site occupancies as shown in Fig. 9. When the five crystal sites are equally occupied by 78 at.% Re, as presented in Fig. 9 (a), the site decomposed DOS of each site near the Fermi level are close to one another, with a relatively higher value on 4*f* site (i.e., CN15 site). Apparently, CN12 sites do not cause high density of states. On the other hand, when CN12 sites are totally occupied by Re, as presented in Fig. 9 (b), it leads to low density of states on CN12 sites. This is against the argument that atoms with half-filled *d* shells would have high density of states when occupying CN12 sites [14].

The present calculations indicate that for the TM-TM binary sigma phase, the constituent atom with more valence electrons or less electron shells would have high density of states near the Fermi level, no matter whether it occupies large or small CN sites. In fact, CN12 sites are preferable for the constituent atom with smaller atomic size, more valence electrons or electron shells [11]. This is related to the tendency of electron loss or gain of the two constituent atoms. For more details see Ref. [11].

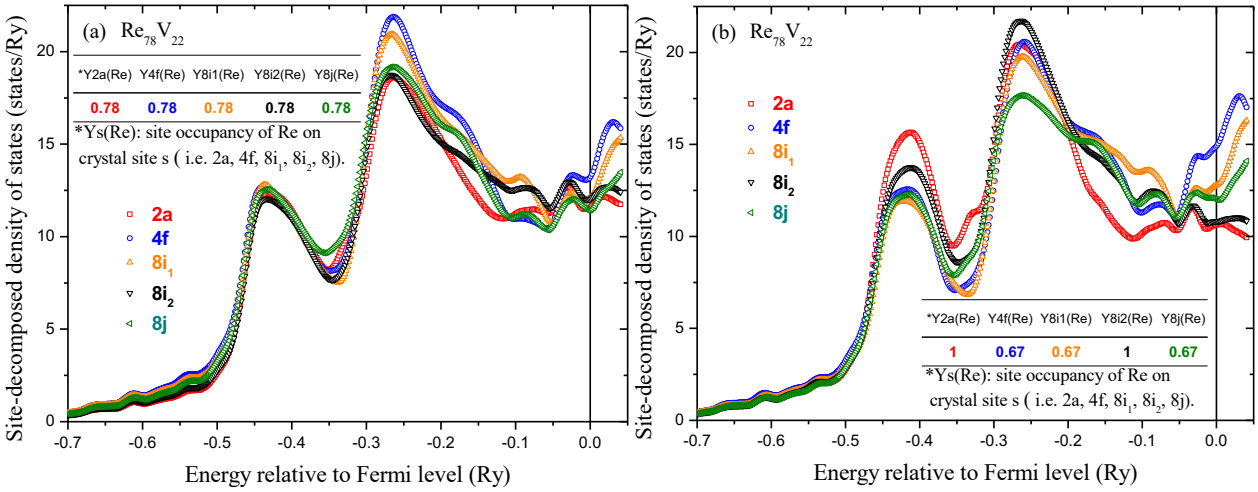

Fig. 9. Site-decomposed DOS for $Re_{78}V_{22}$ sigma compounds from EMTO-CPA calculations. The site

occupancies, shown in the inserted Table in the figure, are artificially hypothetical. The vertical lines indicate the Fermi level. (Color online).

3.3.2. Influence of atomic bonding on molar volume of the sigma phase

The molar volume of the sigma phase varies with the site occupancy even at a fix composition. The influence of site occupancy on molar volume is related to the atomic bonding, and can be described by the volume difference between the completely disordered and ordered state of the $A_{66.7}B_{33.3}$ compounds ($\Delta Vm=V_{disorder}-V_{order}$) [13]. For most sigma phase systems, the volume of the completely ordered state is smaller than that of the disordered one, i.e., ΔVm is positive. The only exception is for Mo-Re system, where ΔVm is negative [13].

It needs to be clarified that for $A_{66.7}B_{33.3}$ in the completely ordered state, large atom A occupies large CN sites (i.e., 4f, 8i_1 and 8j) and small atom B occupies small CN sites (i.e., 2a and 8i_2). Comparing to the disordered state, there are more atoms A on large CN sites, and more atoms B on small CN sites. According to the conclusion drawn in Section 3.2, when constituent A bears more electron shells or less valence electrons than B, the atomic bonding on large CN sites is stronger, and that on small CN sites is weaker for the completely ordered state than for the disordered one. The bonding effect on large CN sites should be more prominent, and thus leads to a smaller ordered volume than the disordered one [13].

On the contrary, when constituent A bears less electron shells or more valence electrons than B, it leads to a larger ordered volume than the disordered one. The only different case is the Mo-Re system, where Mo ($4d^5 5s^1$) has one less electron shell and valence electron than Re ($6d^5 6s^2$). It should be the electron shell factor that makes the volume of the ordered state larger than that of the disordered one [13]. We calculated the site-decomposed DOS for the two $Mo_{48}Re_{52}$ sigma compounds one with site occupancies from the literature (denoted as 'exp') and the other in hypothetically disordered state (denoted as 'dis') as presented in Fig. 10. The results indicate that the atomic bonding on 4f site of the ordered $Mo_{48}Re_{52}$ (exp) is obviously weaker than that of the disordered $Mo_{48}Re_{52}$ (dis), which is caused by the electron shell factor. For other crystal sites (i.e., 2a, 8i_1, 8i_2, 8j), no remarkable difference can be observed due to the competition between the electron shell factor and valence electron one. Thus, a smaller volume for the ordered $Mo_{48}Re_{52}$ (exp) is mainly induced by weaker atomic bonding on 4f site.

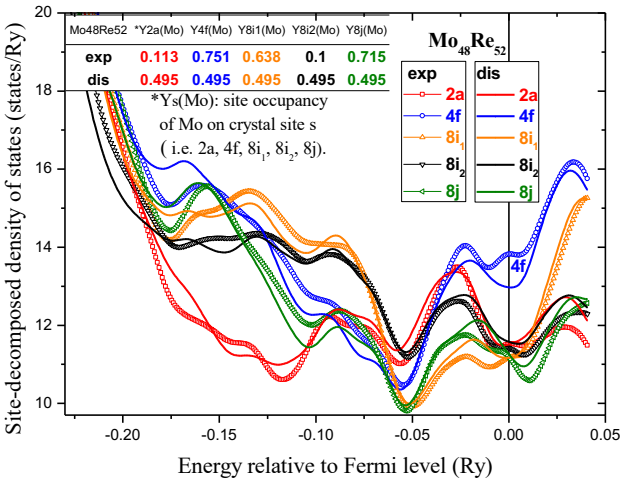

Fig. 10. Site-decomposed DOS for $Mo_{48}Re_{52}$ sigma compounds from EMTO-CPA calculations, where 'exp' and 'dis' indicate compounds with site occupancies from the literature [45] and in hypothetically disordered state, respectively. The vertical line indicates the Fermi level. (Color online).

4. Conclusion

The present work based on the electronic density of states (DOS) and electron localization function (ELF) calculated by using first-principles methods allowed us to clarify the atomic bonding characteristics of the binary sigma phase including *A*-Al (*A*=Nb, Ta) and transition metal systems (TM-TM). The main conclusions are summarized as follows:

1. The atomic bonds of the binary sigma phase exhibit both metallic and covalent characters. The covalent bonding for *A*-Al (*A*=Nb, Ta) is stronger than that for TM-TM.
2. The completely ordered $A_{66.7}Al_{33.3}$ (*A*=Nb, Ta) sigma compounds have higher electronic stability and smaller size mismatch between atom and lattice site than the disordered configurations. Hence, the *A*-Al (*A*=Nb, Ta) sigma compounds are found highly ordered in nature.
3. For a TM-TM sigma compound, the constituent atom, with more electron shells or less valence electrons, holds higher electronic stability. When increasing its atomic occupancy on a specific site, the atomic bonding on the site becomes stronger.
4. For Mo-Re system, the reason why the molar volume of the ordered $Mo_{48}Re_{51}$ compound is larger than that of the disordered $Mo_{48}Re_{51}$ is that the atomic bonds on 4*f* site for the ordered compound are weaker than that of the disordered one. It is dictated by the electron shell factor of the constituents, namely Mo bears less electron shells than Re.

Acknowledgments

This work was supported by National Science Foundation for Young Scientists of China (Grant

number: 51801119). X.-G. Lu acknowledges the High Performance Computing Center of Shanghai University for providing the calculation facility.

References

[1] E.O. Hall, S.H. Algie, The sigma phase, Metall. Rev. 11 (1966) 61–88.

[2] J.-M. Joubert, Crystal chemistry and Calphad modeling of the σ phase, Prog. Mater. Sci. 53 (2008) 528–583. doi:10.1016/j.pmatsci.2007.04.001.

[3] W. Liu, X.-G. Lu, P. Boulet, M.-C. Record, Influence of nearest neighbor atoms and coordination polyhedron on atomic volume of sigma phases, Comput. Mater. Sci. 143 (2018) 308–315. doi:https://doi.org/10.1016/j.commatsci.2017.11.029.

[4] N. Dupin, B. Sundman, A thermodynamic database for Ni-base superalloys, Scand. J. Metall. 30 (2001) 184–192. doi:10.1034/j.1600-0692.2001.300309.x.

[5] R. Mathieu, N. Dupin, J.-C. Crivello, K. Yaqoob, A. Breidi, J.-M. Fiorani, N. David, J.-M. Joubert, CALPHAD description of the Mo–Re system focused on the sigma phase modeling, Calphad. 43 (2013) 18–31. doi:10.1016/j.calphad.2013.08.002.

[6] W. Liu, X.-G. Lu, Y.-L. He, L. Li, Modeling of molar volume of the sigma phase involving transition elements, Comput. Mater. Sci. 95 (2014) 540–550. doi:10.1016/j.commatsci.2014.08.015.

[7] L. Kaufman, H. Bernstein, Computer Calculations of Phase Diagrams, Academic Press, New York, 1970.

[8] N. Saunders, A.P. Miodownik, CALPHAD (calculation of phase diagrams): a comprehensive guide, Pergamon, Oxford ; New York, 1998.

[9] H.L. Lukas, S.G. Fries, B. Sundman, Computational thermodynamics: the CALPHAD method, Cambridge University Press, Cambridge ; New York, 2007.

[10] M.H.F. Sluiter, Prediction of Site Preference and Phase Stability of Transition Metal Based Frank-Kasper Phases, EPD Congr. 2005 Ed. ME Schlesinger TMS Miner. Met. Mater. Soc. (2005). https://www.researchgate.net/publication/266456561_Prediction_of_Site_Preference_and_Phase_Stability_of_Transition_Metal_Based_Frank-Kasper_Phases (accessed September 9, 2017).

[11] W. Liu, X.-G. Lu, P. Boulet, M.-C. Record, Influencing factors of atomic order in the binary sigma phase, Intermetallics. 93 (2018) 6–19. doi:https://doi.org/10.1016/j.intermet.2017.11.006.

[12] G. Bonny, A. Bakaev, D. Terentyev, Y.A. Mastrikov, Elastic properties of the sigma W-Re phase: A first principles investigation, Scr. Mater. 128 (2017) 45–48. doi:10.1016/j.scriptamat.2016.09.039.

[13] W. Liu, X.-G. Lu, P. Boulet, M.-C. Record, H. Wang, Q.-M. Hu, Influence of atomic mixing and atomic order on molar volume of the binary sigma phase, Intermetallics. 98 (2018) 95–105.

[14] J.-C. Crivello, A. Breidi, J.-M. Joubert, χ and σ Phases in Binary Rhenium–Transition Metal Systems: a Systematic First-Principles Investigation, Inorg. Chem. 52 (2013) 3674–3686. doi:10.1021/ic302142w.

[15] W. Liu, X.-G. Lu, P. Boulet, M.-C. Record, Q.-M. Hu, Influence of atomic order on the enthalpy of formation and bulk modulus of the sigma phase, Fluid Phase Equilibria. 495 (2018) 238–243. doi:10.1016/j.fluid.2017.10.006.

[16] J. Cieślak, M. Reissner, W. Steiner, S.M. Dubiel, Magnetic moments and Curie temperatures of σ-FeCr alloys, J. Magn. Magn. Mater. 272–276, Part 1 (2004) 534–535. doi:10.1016/j.jmmm.2003.12.001.

[17] J. Cieślak, B.F.O. Costa, S.M. Dubiel, M. Reissner, W. Steiner, Magnetic ordering above room temperature in the sigma-phase of Fe66V34, J. Magn. Magn. Mater. 321 (2009) 2160–2165. doi:10.1016/j.jmmm.2009.01.005.

[18] C. Berne, A. Pasturel, M. Sluiter, B. Vinet, Ab initio study of metastability in refractory metal based systems, Phys. Rev. Lett. 83 (1999) 1621.

[19] M.H.F. Sluiter, A. Pasturel, Site occupation in the Cr-Ru and Cr-Os σ phases, Phys. Rev. B. 80 (2009). doi:10.1103/PhysRevB.80.134122.

[20] O. Grånäs, P.A. Korzhavyi, A.E. Kissavos, I.A. Abrikosov, Theoretical study of the Mo–Ru sigma phase, Calphad. 32 (2008) 171–176. doi:10.1016/j.calphad.2007.06.001.

[21] L. Vitos, Computational quantum mechanics for materials engineers: the EMTO method and applications, Springer, London, 2007.

[22] L. Vitos, Total-energy method based on the exact muffin-tin orbitals theory, Phys. Rev. B. 64 (2001). doi:10.1103/PhysRevB.64.014107.

[23] P. Soven, Coherent-potential model of substitutional disordered alloys, Phys. Rev. 156 (1967) 809.

[24] B.L. Gyorffy, Coherent-potential approximation for a nonoverlapping-muffin-tin-potential model of random substitutional alloys, Phys. Rev. B. 5 (1972) 2382.

[25] L. Vitos, I.A. Abrikosov, B. Johansson, Anisotropic Lattice Distortions in Random Alloys from First-Principles Theory, Phys. Rev. Lett. 87 (2001). doi:10.1103/PhysRevLett.87.156401.

[26] J.P. Perdew, K. Burke, M. Ernzerhof, Generalized Gradient Approximation Made Simple, Phys. Rev. Lett. 77 (1996) 3865–3868. doi:10.1103/PhysRevLett.77.3865.

[27] G. Kresse, D. Joubert, From ultrasoft pseudopotentials to the projector augmented-wave method, Phys. Rev. B. 59 (1999) 1758.

[28] R.M. Dreizler, E.K.U. Gross, Density Functional Theory, Springer, Berlin, 1998. http://www.springer.com/br/book/9783642861055 (accessed May 18, 2017).

[29] G. Kresse, J. Furthmüller, Efficient iterative schemes for ab initio total-energy calculations using a plane-wave basis set, Phys. Rev. B. 54 (1996) 11169–11186.

[30] J.P. Perdew, Y. Wang, Accurate and simple analytic representation of the electron-gas correlation energy, Phys. Rev. B. 45 (1992) 13244–13249. doi:10.1103/PhysRevB.45.13244.

[31] H.J. Monkhorst, J.D. Pack, Special points for Brillouin-zone integrations, Phys. Rev. B. 13 (1976) 5188–5192. doi:10.1103/PhysRevB.13.5188.

[32] J.-C. Crivello, R. Souques, A. Breidi, N. Bourgeois, J.-M. Joubert, ZenGen, a tool to generate ordered configurations for systematic first-principles calculations: The Cr–Mo–Ni–Re system as a case study, Calphad. 51 (2015) 233–240. doi:10.1016/j.calphad.2015.09.005.

[33] P.J. Brown, J.B. Forsyth, The structure of the σ-phase Nb2Al, Acta Crystallogr. 14 (1961) 362–364.

[34] A. Boulineau, J.-M. Joubert, R. Černý, Structural characterization of the Ta-rich part of the Ta–Al system, J. Solid State Chem. 179 (2006) 3385–3393. doi:10.1016/j.jssc.2006.07.001.

[35] L.E. Edshammar, B. Holmbery, The σ-phase Ta2Al, Acta Chem Scand. 14 (1960) 1219–1220.

[36] Q.-M. Hu, L. Vitos, R. Yang, Theoretical investigation of the ω -related phases in TiAl − Nb /Mo alloys, Phys. Rev. B. 90 (2014). doi:10.1103/PhysRevB.90.054109.

[37] P. Ravindran, B. Johansson, O. Eriksson, Electronic structure, chemical bonding, phase stability, and ground-state properties of YNi 2 − x (C o / C u) x B 2 C, Phys. Rev. B. 58 (1998) 3381–3393. doi:10.1103/PhysRevB.58.3381.

[38] Q.-M. Hu, R. Yang, D.S. Xu, Y.L. Hao, D. LI, Geometric and electronic structure of Ti2AlX (X=V, Nb, or Ta), Phys. Rev. B. 68 (2003) 054102.

[39] J. Zou, C.L. Fu, Structural, electronic, and magnetic properties of 3 *d* transition-metal aluminides with equiatomic composition, Phys. Rev. B. 51 (1995) 2115–2121. doi:10.1103/PhysRevB.51.2115.

[40] M. Kohout, Wagner Frank Richard, Y. Grin, Electron localization function for transition-metal compounds, Theor. Chem. Acc. 108 (2002) 150–156.

[41] S. Shi, L. Zhu, H. Zhang, Z. Sun, Segregation effects of Y, Ti, Cr and Si on the intergranular fracture of niobium, J. Alloys Compd. 711 (2017) 637–642.

[42] A. Savin, R. Nesper, S. Wengert, T.E. Fassler, ELF: The Electron Localization Function, Angew Chem Im Ed Engl. 36 (1997) 1808–1832.

[43] L. Gao, J. Zhou, Z. Sun, R. Chen, E. Han, Electronic origin of the anomalous solid solution hardening of Y and Gd in Mg: A first-principles study, Chin. Sci. Bull. 56 (2011) 1038–1042.

[44] J. Cieślak, M. Reissner, S.M. Dubiel, J. Wernisch, W. Steiner, Influence of composition and annealing conditions on the site-occupation in the σ-phase of Fe–Cr and Fe–V systems, J. Alloys Compd. 460 (2008) 20–25. doi:10.1016/j.jallcom.2007.05.098.

[45] S.A. Farzadfar, M. Levesque, M. Phejar, J.-M. Joubert, Thermodynamic assessment of the Molybdenum–Rhenium system, Calphad. 33 (2009) 502–510. doi:10.1016/j.calphad.2009.02.001.